

Experimental cross sections for electron-impact ionization of chromium ions: Cr^{6+} , Cr^{7+} , Cr^{8+} , and Cr^{10+}

M. Sataka

Department of Physics, Japan Atomic Energy Research Institute, Tokai-mura, Ibaraki, 319-11 Japan

S. Ohtani

Institute of Plasma Physics, Nagoya University, Chikusa-ku, Nagoya, 464 Japan

D. Swenson

*Joint Institute for Laboratory Astrophysics, Boulder, Colorado 80309-0440
and Oak Ridge National Laboratory, Oak Ridge, Tennessee 37831-6372*

D. C. Gregory

Physics Division, Oak Ridge National Laboratory, Oak Ridge, Tennessee 37831-6372

(Received 19 September 1988)

Absolute cross sections have been measured from below threshold to 1500 eV for electron-impact single ionization of chromium ions in initial charge states $6+$, $7+$, $8+$, and $10+$. The measurements utilized the Oak Ridge National Laboratory Electron Cyclotron Resonance ion source and electron-ion crossed-beams apparatus. The lowest three charge states, which have $3s^23p^n$ ground-state electron configurations, all exhibit ionization onsets at lower energies than expected for ground-state ions, indicating the presence of ions in metastable configurations in the incident beams. Significant contributions to the total cross sections by excitation autoionization are observed for each ion. The present measurements are compared to calculations of direct ionization from the Lotz formula, and the Cr^{10+} measurements are compared to previous data for the isoelectronic ion Ni^{14+} .

I. INTRODUCTION

Electron-impact ionization of ions is of basic interest in various areas of research including plasma physics and astrophysics.¹⁻⁴ Especially in fusion research, accurate data for ionization of impurity ions by electrons are indispensable for modeling power balance, charge-state distributions, impurity composition, and for spectroscopic diagnostics.^{5,6} Recently the data needs for fusion have focused on the low- and intermediate-mass elements, especially those elements found in vacuum-wall materials such as stainless steel.⁷ Chromium is a common constituent of vacuum-wall materials for modern plasma facilities, and is often observed as a plasma impurity in concentrations higher than would be expected from the chemical composition of the construction materials. The ionization cross sections for multiply ionized chromium ions are thus of importance for precise modeling and diagnostics of fusion-related and other plasmas.

A number of ionization measurements have been made for ions of metallic elements. However, because of difficulties producing these ions, the ionization stages used in crossed-beams experiments have been restricted until recently to initial charge states $3+$ or lower.⁸⁻¹⁶ Electron-impact single-ionization cross sections have now been measured for multiply charged Fe (Refs. 17 and 18) and Ni (Ref. 19) ions with initial charge states between $5+$ and $15+$. Distorted-wave calculations have been

made by Pindzola and co-workers²⁰⁻²² for single ionization of all members of the Fe isonuclear sequence. They have taken into consideration direct ionization and excitation-autoionization for ground-state and metastable configurations. These calculations and measurements provide a good database for comparison with other isoelectronic ions of low- and intermediate- Z elements.

For chromium, ionization cross sections have been measured on singly charged ions by Man *et al.*,¹⁶ but no previous measurements are available for multiply charged chromium ions. There are no distorted-wave or close-coupling calculations for chromium ions except for Na-like Cr^{13+} , for which Griffin *et al.*²⁰ included a detailed study of the contribution of excitation autoionization to the total cross section.

We have measured absolute single-ionization cross sections for electron impact on chromium ions with initial charge states $6+$, $7+$, $8+$, and $10+$ in the energy range from below threshold to 1500 eV. The experimental arrangement and uncertainties are briefly presented in Sec. II. The experimental results are presented and discussed in Sec. III. Finally, the conclusions are presented in Sec. IV.

II. EXPERIMENTAL TECHNIQUE

A detailed description of the apparatus has been reported elsewhere,⁷ so only a brief discussion of the experi-

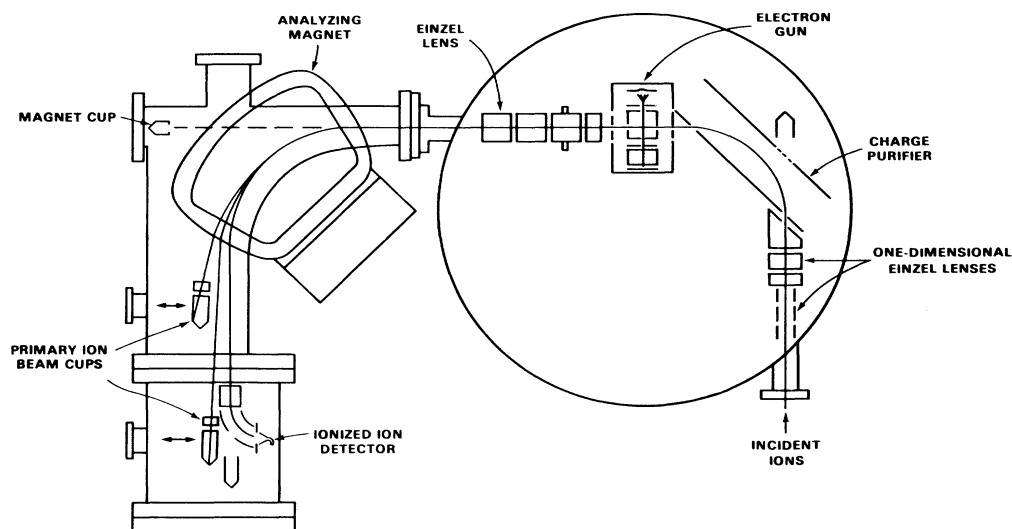


FIG. 1. Schematic of the ORNL crossed-beams collision chamber and post-collision magnetic charge analyzer.

mental arrangement and uncertainties is given here. Chromium ions were extracted from the Oak Ridge National Laboratory Electron Cyclotron Resonance (ORNL-ECR) source,²³ where the ions were produced by inserting a thin Inconel foil (consisting mainly of nickel and chromium) into the edge of the ECR plasma. We were unable to extract and analyze a pure beam of Cr^{9+} ions from the source due to the presence of a significant component of impurity $^{58}\text{Ni}^{10+}$ ions with almost exactly the same mass-to-charge ratio as the desired beam. The ions were extracted from the source with a 10 kV accelerating potential, mass analyzed by a double-focusing 90° magnet, and transported to the ultrahigh vacuum (9×10^{-10} Torr) chamber shown in Fig. 1. In this chamber, the ions were focused by one-dimensional Einzel lenses, charge purified by a 90° electrostatic deflector, and finally introduced into the collision region.

The electron beams were produced by an electron gun very similar to that described by Taylor *et al.*²⁴ The electron beams were magnetically confined and collected in a Faraday cup which was designed to minimize the back-scattered electrons. The electrons were chopped electrostatically so that signal events could be separated from background. The energy spread in the electron beam was estimated to be less than 2 eV.²⁵ After passing through the interaction region, the ions were magnetically charge selected by the double-focusing 90° analyzing magnet. Ions with the incident charge were monitored by collection in a Faraday cup. The ionized ions were deflected out of the collision plane by an electrostatic analyzer and counted in a channel electron multiplier (CEM). Electron- and ion-beam profiles were measured for each data point using a narrow slit and the geometrical overlap was determined. The pulse-height distribution from the CEM was also measured in order to correct for pulses which were not counted by the electronics. Careful absolute measurements of all these quantities al-

lowed us to determine absolute cross sections at each energy studied. Typical experimental parameters are listed for each target ion in Table I.

Uncertainties listed and plotted in this report are relative only at one-standard-deviation (1-s.d.) level and are dominated by counting statistics. The reliability of the shape of the cross-section curve and the relative values of individual points may be judged based on the relative uncertainty. The relative uncertainties for the different charge states range from 1% to 6% for typical measurements near the peak cross sections. Additional systematic uncertainties (which may effect the magnitude of the entire cross-section curve) come mainly from the measurements of the beam overlaps, electron and ion currents

TABLE I. Typical experimental parameters at approximately twice the ionization threshold.

	Cr^{6+}	Cr^{7+}	Cr^{8+}	Cr^{10+}
Electron energy (eV)	300	375	400	550
Electron current (mA)	1.1	1.4	1.6	2.1
Ion current (particle-nA)	5.7	7.1	6.6	4.6
Form factor (cm)	0.48	0.48	0.47	0.45
Background count rate (Hz)	18	15	82	125
Signal count rate (Hz)	75	56	34	12
Cross section (10^{-18} cm ²)	7.3	3.7	2.2	0.92

and velocities, the ion transmission from the collision volume to the detector [taken as $(98 \pm 2)\%$], and the electronic sensitivity (usually 97%). Total absolute uncertainties for typical measurements near the peak cross sections (the quadrature sum of all relative and systematic uncertainties) are between 8% and 10% at 90% confidence level (equivalent to two statistical standard deviations). Previous publications discuss the error analysis in more detail.^{17,26}

III. RESULTS AND DISCUSSION

A. Cr^{6+} , Cr^{7+} , and Cr^{8+}

The measured cross sections for Cr^{6+} , Cr^{7+} , and Cr^{8+} are listed in Table II and plotted in Figs. 2–4. The uncertainties listed and plotted are 1-s.d. relative only and are dominated by counting statistics. Total absolute uncertainties for typical measurements near the peak cross sections are less than 8% for Cr^{6+} and Cr^{7+} , and 9% for Cr^{8+} at the 2-s.d. level. Also shown in the figures are results from the Lotz semiempirical formula²⁷ for direct ionization of ions in the ground states ($3s^23p^n$; $n = 6, 5,$ and 4 with increasing charge, lower curves) and metastable configurations ($3s^23p^{n-1}3d$, upper curves). The Lotz formula is expected to be a good estimate of direct ionization for these charge states and this mass. For similar charge states in iron^{17,18} and nickel¹⁹ ions, the Lotz predictions were within 20% of the more accurate distorted-wave calculations for direct ionization. We use the Lotz predictions in this case, in the absence of more accurate calculations, as a basis for estimating the importance of indirect effects in these measurements. The threshold energies for ionization of the $3d$, $3p$, and $3s$ subshells were calculated using the relativistically corrected

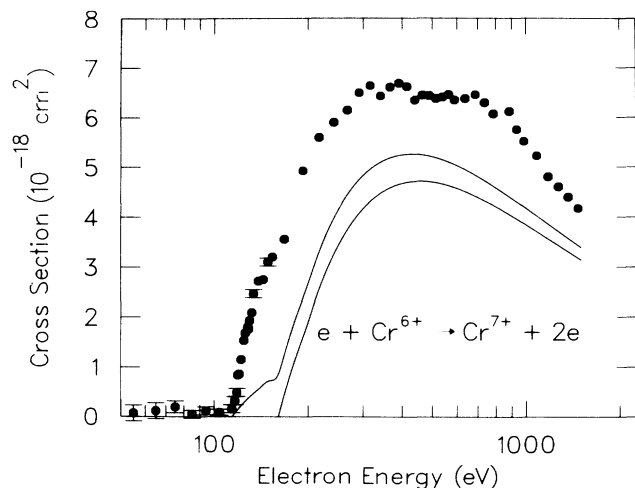


FIG. 2. Electron-impact ionization cross section of Cr^{6+} . The closed circles are the present measurements; relative uncertainties for experimental data are plotted at the one-standard-deviation level where they are larger than the plotted circles. The solid curves are Lotz calculations (Ref. 27) for direct ionization from the ground- (lower curve) and metastable-state configurations (upper curve).

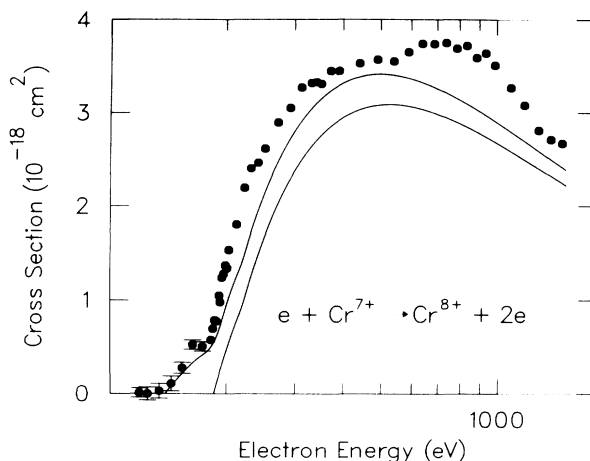


FIG. 3. Electron-impact ionization cross section of Cr^{7+} . The notation is the same as for Fig. 2.

Hartree-Fock atomic structure program developed by Cowan.²⁸ The calculated threshold energies are listed in Table III.

The shapes of these three cross section curves are similar to each other. Two common characteristics of the data sets are outstanding. First, the threshold energies in each case are lower than expected for ground-state-configuration ions ($3s^23p^n$). This is the signature of metastable components in the incident ion beams. In each case, the onset energies agree with those expected for ionization from the first-excited configurations ($3s^23p^{n-1}3d$), some levels of which are metastable. Next, over the entire energy range measured, the Lotz calculations for direct ionization from the ground state considerably underestimate the measured cross sections. Good agreement is found, however, between the measurements and calculations for direct ionization from the metastable configurations of Cr^{7+} and Cr^{8+} at energies below the ground-state configuration ionization onset.

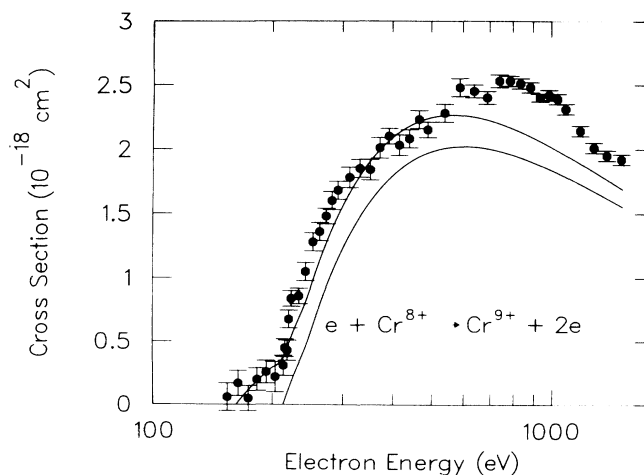


FIG. 4. Electron-impact ionization cross section of Cr^{8+} . The notation is the same as for Fig. 2.

TABLE II. Electron-impact ionization cross sections for Cr^{6+} , Cr^{7+} , Cr^{8+} , and Cr^{10+} . Uncertainties are one-standard-deviation relative only.

Cr^{6+}				Cr^{7+}			
Energy (eV)	Cross section (10^{-18} cm^2)	Energy (eV)	Cross section (10^{-18} cm^2)	Energy (eV)	Cross section (10^{-18} cm^2)	Energy (eV)	Cross section (10^{-18} cm^2)
55.0	0.07±0.10	217	5.59±0.05	118.9	0.01±0.05	371	3.45±0.04
65.0	0.11±0.16	242	5.97±0.06	124.5	0.00±0.07	391	3.45±0.01
75.1	0.20±0.12	267	6.14±0.05	134.5	0.03±0.08	440	3.53±0.03
85.0	0.05±0.08	291	6.49±0.03	143.7	0.11±0.08	489	3.57±0.03
94.2	0.11±0.08	316	6.63±0.04	153.8	0.28±0.06	539	3.55±0.03
104.3	0.10±0.06	341	6.42±0.07	163.7	0.53±0.05	589	3.65±0.04
114.2	0.18±0.08	366	6.60±0.03	173.9	0.51±0.05	639	3.74±0.03
116.5	0.31±0.08	391	6.68±0.03	183.0	0.58±0.04	686	3.74±0.01
118.2	0.50±0.08	415	6.61±0.04	185.5	0.70±0.05	737	3.75±0.02
118.8	0.84±0.09	440	6.34±0.05	187.8	0.79±0.04	786	3.69±0.02
120.4	0.88±0.08	465	6.44±0.04	189.3	0.78±0.06	833	3.72±0.03
122.0	1.17±0.08	489	6.43±0.07	191.7	1.05±0.05	883	3.59±0.03
124.5	1.55±0.05	514	6.37±0.04	193.1	0.98±0.08	932	3.64±0.03
125.9	1.71±0.08	539	6.40±0.05	195.3	1.24±0.04	983	3.51±0.02
128.3	1.84±0.08	564	6.45±0.04	197.1	1.28±0.05	1081	3.27±0.02
129.0	1.81±0.08	589	6.54±0.04	199.2	1.37±0.05	1171	3.08±0.03
129.9	1.93±0.08	637	6.37±0.04	200.8	1.34±0.05	1275	2.81±0.02
132.1	2.05±0.08	687	6.45±0.03	202.9	1.53±0.04	1370	2.71±0.02
134.2	2.54±0.08	736	6.29±0.03	213	1.80±0.04	1465	2.67±0.02
139.0	2.81±0.08	785	6.05±0.02	223	2.19±0.05		
143.6	2.80±0.05	883	6.11±0.04	232	2.40±0.04		
148.9	3.20±0.08	931	5.75±0.04	242	2.46±0.06		
153.7	3.22±0.04	982	5.55±0.04	252	2.61±0.05		
158.0	3.50±0.04	1080	5.26±0.04	272	2.89±0.04		
163.4	3.60±0.04	1173	4.80±0.04	292	3.05±0.05		
168.1	3.73±0.04	1267	4.60±0.03	312	3.27±0.04		
173.6	4.18±0.04	1363	4.39±0.04	331	3.32±0.04		
178.2	4.77±0.04	1460	4.17±0.02	341	3.33±0.04		
192.8	4.96±0.03			351	3.31±0.04		

Distinct breaks in the slopes of the data at the ground-state ionization thresholds for Cr^{7+} and Cr^{8+} imply the dominance of direct ionization, in which case the good agreement with metastable direct ionization theory indicates that the incident ion beams are almost pure metastable (90% or more). For Cr^{6+} , the calculation for excited ions still significantly underestimates the measured cross section. The difference near threshold for Cr^{6+} is attributed to significant contributions to the total cross sections by excitation of 3s electrons from the metastable configuration followed by autoionization. The corresponding transitions from the ground-state configuration ion are bound, as was the case for the isoelectronic iron ion.^{21,22} Many of the 3s-*nl* excitations in metastable Cr^{7+} and Cr^{8+} are also bound, and indirect ionization decreases rapidly with increasing charge, as was predicted for the isoelectronic iron ions, Fe^{9+} and Fe^{10+} . We were unable to significantly alter the metastable fractions of the extracted ion beams by changing source conditions.

The added enhancements observed for these three ions at energies higher than 500 eV are attributed to 2s-*nl* and 2p-*nl* excitations from the ground and/or metastable configurations followed by autoionization. For the isoelectronic iron ions, these features were predicted and

were dominated by the 2p-3d transition, with small contributions from numerous other transitions.²¹ A similar interpretation should be valid for the isoelectronic ions in this study.

B. Cr^{10+}

The measured cross sections for Cr^{10+} are listed in Table II and plotted in Fig. 5. The uncertainties listed and plotted are 1-s.d. values (relative only) and are dominated by counting statistics. The total absolute uncertainty for a typical measurement near the peak cross section is 10% at the 2-s.d. level. The measured cross sections are compared in the figure with the Lotz predictions²⁷ for direct ionization from the ground-state configuration ($3s^2 3p^2$). The threshold energies for ionization of the 3s and 3p subshells were calculated using Cowan's relativistic Hartree-Fock (HFR) code.²⁸ The energies are listed in Table III.

The observed ionization threshold energy is consistent with the ground-state-configuration ionization energy. The incident Cr^{10+} ion beam is observed to contain a negligible fraction of metastables, in contrast to the cases described above. The Lotz cross section is in good agree-

TABLE II. (Continued).

Cr^{8+}				Cr^{10+}			
Energy (eV)	Cross section (10^{-18} cm^2)	Energy (eV)	Cross section (10^{-18} cm^2)	Energy (eV)	Cross section (10^{-18} cm^2)	Energy (eV)	Cross section (10^{-18} cm^2)
154.0	0.06±0.11	391	2.10±0.06	242	-0.06±0.08	736	1.24±0.04
164.0	0.17±0.11	415	2.03±0.08	252	-0.01±0.07	786	1.29±0.03
174.1	0.05±0.10	440	2.08±0.07	262	-0.04±0.07	833	1.23±0.04
183.2	0.20±0.09	465	2.23±0.07	272	0.13±0.09	882	1.32±0.04
193.3	0.26±0.09	489	2.15±0.06	282	0.41±0.13	932	1.22±0.04
203.1	0.22±0.12	539	2.28±0.07	292	0.29±0.11	982	1.25±0.03
213	0.31±0.08	589	2.49±0.01	312	0.36±0.09	1032	1.14±0.05
215	0.45±0.07	638	2.45±0.05	331	0.52±0.09	1078	1.17±0.03
218	0.43±0.08	688	2.40±0.05	351	0.50±0.08	1174	1.10±0.07
220	0.68±0.07	738	2.53±0.05	371	0.70±0.08	1269	1.09±0.06
223	0.84±0.06	786	2.53±0.04	391	0.71±0.06	1364	0.97±0.05
233	0.86±0.06	834	2.51±0.04	415	0.62±0.07	1461	0.90±0.05
243	1.05±0.07	883	2.48±0.04	440	0.72±0.09		
253	1.28±0.07	932	2.40±0.03	465	0.71±0.07		
263	1.36±0.07	983	2.42±0.04	489	0.84±0.05		
273	1.48±0.06	1032	2.39±0.04	514	0.80±0.06		
282	1.60±0.07	1081	2.31±0.04	539	0.83±0.05		
292	1.68±0.07	1175	2.14±0.04	564	0.96±0.05		
312	1.78±0.08	1271	2.01±0.04	588	1.03±0.02		
331	1.85±0.07	1369	1.95±0.04	613	1.11±0.05		
351	1.84±0.08	1489	1.92±0.04	638	1.18±0.04		
371	2.01±0.08			663	1.19±0.04		

ment with the measured cross sections in the energy region below 500 eV, where a sudden increase in cross section is observed. The onset of indirect ionization clearly appears, in contrast to the lower charge states where

numerous individual transitions contribute to a broad enhancement of the cross section. The primary contribution in this case is the $2p$ - $3d$ excitation followed by autoionization. Based on the calculations of Pindzola and

TABLE III. Ionization potentials for Cr^{6+} , Cr^{7+} , Cr^{8+} , and Cr^{10+} calculated using the distorted-wave code developed by Cowan (Ref. 28).

Ion	Configuration	Subshell	Configuration-average ionization potential (eV)
Cr^{6+}	$3s^23p^6$	$3p$	160.5
		$3s$	198.2
	$3s^23p^53d$	$3d$	114.0
		$3p$	161.1
		$3s$	196.4
Cr^{7+}	$3s^23p^5$	$3p$	185.9
		$3s$	221.8
	$3s^23p^43d$	$3d$	138.8
		$3p$	186.3
		$3s$	219.9
Cr^{8+}	$3s^23p^4$	$3p$	212.2
		$3s$	246.3
	$3s^23p^33d$	$3d$	164.7
		$3p$	212.5
		$3s$	244.2
Cr^{10+}	$3s^23p^2$	$3p$	267.8
		$3s$	297.9

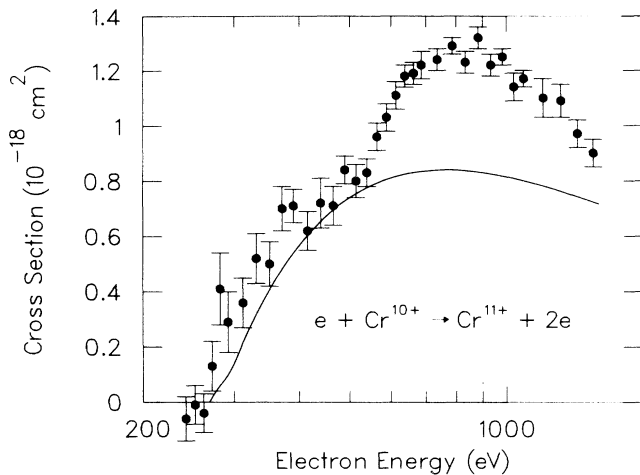


FIG. 5. Electron-impact ionization cross section of Cr^{10+} . The closed circles are the present measurements; relative uncertainties for experimental data are plotted at the one-standard-deviation level. The solid curve is a Lotz calculation (Ref. 27) for direct ionization from the ground-state configuration ($3s^23p^2$).

co-workers^{21,22} for Fe ions, important contributions are also expected due to the $2p$ - $3p$ and $2s$ - $3d$ excitations. The energy range over which this feature increases is consistent with the excitation onset energies for these transitions.

Based on classical scaling, cross sections Q for direct ionization may be represented in terms of the ionization energy (I) as a function of the energy in threshold units E/I by a universal curve

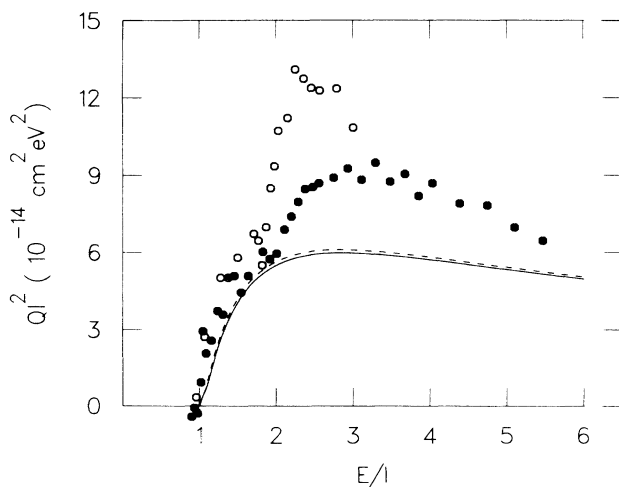


FIG. 6. Reduced cross sections (I^2Q) for Cr^{10+} vs electron energy in $3p$ threshold energy units (E/I). The closed circles are the present data. The open circles are the reduced data for Ni^{14+} (from Ref. 19). The solid and dashed curves are Lotz calculations (Ref. 27) for Cr^{10+} and Ni^{14+} , respectively.

$$I^2Q = f(E/I) . \quad (1)$$

Cross sections for isoelectronic ions may be conveniently compared using this simple scaling. Based on quantum-mechanical considerations,²⁹⁻³² the formula should include dependence on the atomic number Z . However, it is possible to compare the cross sections for ions close in atomic number without considering the Z dependence.

The reduced cross sections I^2Q for Cr^{10+} are plotted in Fig. 6 as a function of electron energy in $3p$ ionization threshold units. They are compared to the reduced data for the isoelectronic Ni^{14+} ion, which has recently been measured by Wang *et al.*¹⁹ Reduced Lotz cross sections for Cr^{10+} and Ni^{14+} are also shown in Fig. 6.

In comparing the reduced data for the two isoelectronic ions, several features are worthy of mention: (a) no contributions are observed due to metastable ions in the incident beams; (b) the reduced data are in good agreement in the energy region from threshold to the onset of indirect ionization; (c) in the energy range above the indirect ionization onset, the peak cross sections appear to be different, implying that the contributions of excitation autoionization involving inner-shell electrons do not scale by this relationship; (d) the dip observed in the Ni^{14+} reduced cross section curve just below the indirect ionization onset is not seen in the Cr^{10+} data. Characteristics (b) and (c) are also observed in comparing the reduced cross section data of Cr^{7+} and Cr^{8+} with data^{17,18} for the isoelectronic iron ions. The present data are also consistent with previous ionization studies in that indirect ionization becomes more important in comparison with direct ionization as the ionic charge increases.

IV. CONCLUSIONS

Measurements have been made and presented of cross sections for electron-impact ionization of chromium ions with initial charges $6+$, $7+$, $8+$, and $10+$. The cross-section curves of the lowest three charge states are similar to each other. The onset energies for Cr^{6+} , Cr^{7+} , and Cr^{8+} are lower than expected for ions in the ground state and agree with energies predicted for metastable ions. Comparisons of the measured cross sections with Lotz calculations for direct ionization indicate a significant, but decreasing, indirect ionization contribution as a function of increasing charge.

The measured data for Cr^{10+} indicates a negligible fraction of metastable ions in the incident beam. The onset of indirect ionization appears clearly in the cross section curve. The measured cross sections are in good agreement with Lotz cross sections for ground-state ions in the energy region between the threshold and the onset of the indirect ionization. There is also agreement between the reduced cross sections for Cr^{10+} and the isoelectronic Ni^{14+} in the same energy range. At energies above the onset of indirect ionization, the peak value of the reduced cross section for Ni^{14+} is significantly higher than that of Cr^{10+} , implying that inner-shell excitation followed by autoionization becomes relatively

more important along an isoelectronic sequence as the ionic charge increases.

ACKNOWLEDGMENTS

The authors acknowledge valuable interactions with R. A. Phaneuf and F. W. Meyer during this project. Tech-

nical assistance from J. W. Hale is also acknowledged. This work was supported in part by the Office of Fusion Energy, U.S. Department of Energy, under Contract No. DE-AC05-84OR21400 with Martin Marietta Energy Systems, Inc.

-
- ¹A. Dalgarno, in *Physics of Ion-Ion and Electron-Ion Collisions* (Plenum, New York, 1983), pp. 1–36.
- ²D. E. Post, in Ref. 1, pp. 37–99.
- ³David H. Crandall, *Nucl. Instrum. Methods* **214**, 129 (1983).
- ⁴R. A. Phaneuf, in *Atomic Processes in Electron-Ion and Ion-Ion Collisions*, edited by F. Brouillard (Plenum, New York, 1986), pp. 117–156.
- ⁵D. Palumbo, *Phys. Scr.* **23**, 69 (1981).
- ⁶R. C. Isler, *Nucl. Fusion* **24**, 1599 (1984).
- ⁷C. F. Barnett, *Nucl. Instrum. Methods* **214**, 1 (1983).
- ⁸R. A. Falk, G. H. Dunn, D. C. Gregory, and D. H. Crandall, *Phys. Rev. A* **27**, 762 (1983).
- ⁹R. G. Montague, M. J. Diserens, and M. F. A. Harrison, *J. Phys. B* **17**, 2085 (1984).
- ¹⁰R. G. Montague and M. F. A. Harrison, *J. Phys. B* **17**, 2707 (1984).
- ¹¹D. W. Mueller, T. J. Morgan, G. H. Dunn, D. C. Gregory, and D. H. Crandall, *Phys. Rev. A* **31**, 2905 (1985).
- ¹²R. G. Montague and M. F. A. Harrison, *J. Phys. B* **18**, 1419 (1985).
- ¹³M. J. Diserens, A. C. H. Smith, and M. F. A. Harrison, *J. Phys. B* **21**, 2129 (1988).
- ¹⁴D. C. Gregory and A. M. Howald, *Phys. Rev. A* **34**, 97 (1986).
- ¹⁵K. F. Man, A. C. H. Smith, and M. F. A. Harrison, *J. Phys. B* **20**, 1351 (1987).
- ¹⁶K. F. Man, A. C. H. Smith, and M. F. A. Harrison, *J. Phys. B* **20**, 2571 (1987).
- ¹⁷D. C. Gregory, F. W. Meyer, A. Müller, and P. Defrance, *Phys. Rev. A* **34**, 3657 (1986).
- ¹⁸D. C. Gregory, L. J. Wang, F. W. Meyer, and K. Rinn, *Phys. Rev. A* **38**, 3256 (1987).
- ¹⁹L. J. Wang, K. Rinn, and D. C. Gregory, *J. Phys. B* **21**, 2117 (1988).
- ²⁰D. C. Griffin, M. S. Pindzola, and C. Bottcher, *Phys. Rev. A* **36**, 3642 (1987).
- ²¹M. S. Pindzola, D. C. Griffin, C. Bottcher, S. M. Younger, and H. T. Hunter, Oak Ridge National Laboratory Report No. ORNL/TM-10297, 1987 (unpublished); *Nucl. Fusion, Special Supplement* 1987, p. 21.
- ²²M. S. Pindzola, D. C. Griffin, and C. Bottcher, *Phys. Rev. A* **34**, 3668 (1986).
- ²³F. W. Meyer, *Nucl. Instrum. Methods Phys. Res. B* **9**, 532 (1985).
- ²⁴P. O. Taylor, K. T. Dolder, W. E. Kauppila, and G. H. Dunn, *Rev. Sci. Instrum.* **45**, 538 (1974).
- ²⁵D. S. Belic, R. A. Falk, G. H. Dunn, D. Gregory, C. Cisneros, and D. H. Crandall, *Bull. Am. Phys. Soc.* **26**, 1315 (1981).
- ²⁶D. H. Crandall, R. A. Phaneuf, and P. O. Taylor, *Phys. Rev. A* **18**, 1911 (1978).
- ²⁷W. Lotz, *Z. Phys.* **206**, 205 (1967); **216**, 241 (1968); **220**, 466 (1969).
- ²⁸R. D. Cowan, *The Theory of Atomic Structure and Spectra* (University of California Press, Berkeley, 1981).
- ²⁹E. J. McGuire, *Phys. Rev. A* **16**, 73 (1977).
- ³⁰D. L. Moores, L. B. Golden, and D. H. Sampson, *J. Phys. B* **13**, 385 (1980).
- ³¹S. M. Younger, *Phys. Rev. A* **24**, 1278 (1981).
- ³²S. M. Younger, *Phys. Rev. A* **25**, 3396 (1982).